EXPERIMENTAL STUDY ON HEAT TRANSFER CHARACTERISTICS OF HIGH-TEMPERATURE HEAT PIPE

Bowen XU[1], Jinwang LI[1*, 2], Ningxiang LU[1], Changji WANG[1]

1 College of Astronautics, Nanjing University of Aeronautics and Astronautics, Nanjing 211106, China

2 Jiangsu Province Key Laboratory of Aerospace Power System, Nanjing 210096, China

[*] Corresponding author; E-mail: ljw@nuaa.edu.cn

High-temperature heat pipes have broad application prospects in terms of thermal protection of hypersonic aircraft and cooling of space nuclear reactors. In this paper, a high-temperature heat pipe heat transfer performance experimental platform is built to study the heat transfer performance of high-temperature heat pipes at different inclination angles. A heat transfer network model of high-temperature heat pipes containing non-condensable gas is established to analyze the influence of non-condensable gas. The results show that as the inclination angle of the heat pipe increases, the start-up time of the heat pipe does not change. The heat transfer performance is best when the inclination angle is 30°. High-temperature heat pipes containing non-condensable gas will reduce the effective length of the high-temperature heat pipe, increase the thermal resistance, and reduce the heat transfer performance. The high-temperature heat pipe analysis model with non-condensable gas established in this paper can be used to predict the heat transfer performance of high-temperature heat pipes containing non-condensable gas.

Key words*: High-temperature heat pipe, heat transfer, inclination angle, heating power, non-condensable gas*

1. Introduction

High-temperature heat pipes are one of the hot research directions in the field of heat pipes, and they have broad application prospects in terms of thermal protection of hypersonic aircraft, cooling of space nuclear reactors and solar energy utilization [1-3]. However, due to the high working temperature of high-temperature heat pipes, its working fluid, wick, and pipe materials have certain special characteristics. Some of the existing laws and properties in medium and low temperature heat pipes may no longer be applicable to high-temperature heat pipes. The experimental conditions of heat pipes are relatively harsh and there are still insufficient researches on the performance of high-temperature heat pipes.

There are some basic heat pipe experiments: Thomas et al. [4] explored the monel / water heat pipes as an option for operation up to 300°C. Life tests of up to 30000 h have

shown good compatibility at 250°C. Rongji et al. [5] investigated the dynamic response of pulsating heat pipes and the results shows that the dynamic response time constant of pure fluids decreases when the quantity of the liquid working fluid in the pulsating heat pipe decreases with the increase in heating power. Sriram et al. [6] investigate the heat transfer performance of pulsating heat pipe using self-rewetting fluids of high carbon alcohols. The latent heat of vaporization plays an important role in the heat transfer performance of pulsating heat pipe. It was observed that the high carbon alcohols showed a decrease in the latent heat of vaporization. S.U.N[7] according to the thermodynamic model established the heat generation model and coupled heat transfer model of the battery with multi-stage heating method based on flat heat pipes. Different heating powers are assigned to different heating points and the total heating power is kept constant. Mahdavi et al. [8] investigated the effect of the working fluid fill volume, inclination angle, and heat input on the equivalent thermal resistance of the heat pipe. Yu et al. [9] investigated the start-up performance of high-temperature heat pipe through experiments and the results show that the inclination angle has an obvious influence on the start-up characteristics of high-temperature heat pipe. When the heat pipe is placed horizontally, the temperature rise rate of the heat insulation part "lags". Ding et al. [10] carried out an experimental study on the specific structure of the high-temperature heat pipe. The results show that the higher the input power, the shorter the start-up time of the high-temperature heat pipe and the inclination angle of the heat pipe has little effect on the starting performance. The inclination angle increases from 0° to 90° and the steam flow transition temperature of the heat pipe is the same, the start-up time is the same, and the equilibrium temperature is the same. Shen et al. [11] carried out experimental research on heat transfer characteristics of high-temperature heat pipe with special structure under different heating conditions. The results show that the starting time and temperature of constant heating power are basically equal to that of periodic alternating power with the same average power. Nina et al. [12] investigated the high-temperature heat pipes with a ceramic container consisting out of sintered silicon carbide (SSiC) and with zinc as working fluid. The results show that the best performance is reached with a filling amount of 100 g zinc as working fluid, which comes up to a filling height of about 11% of the total heat pipe length under liquid conditions.

At the same time, the life of heat pipe is a hot topic in the research of heat pipe. In many heat pipe experiments, researchers found that the generation of non-condensable gas (NCG) in the heat pipe is considered as one of the main factors affecting the life of heat pipe [13]. The researchers found that the existence of a certain amount of non-condensable gas is helpful to the start-up stage of high-temperature heat pipe. Ochterbeck et al. [14] investigated the effect of non-condensable gas on the start-up of heat pipe by establishing a one-dimensional transient model. The freezing start-up of high-temperature heat pipe becomes easier after adding non condensable gas. However, the existence of non-condensable gas may cause the start-up difficulty or failure of the loop heat pipe [15]. By using the characteristic of non-condensable gas affecting the thermal resistance of high-temperature heat pipe, a variable heat conduction heat pipe (VCHP) can be made [16], or the working temperature of LHP can be actively and accurately controlled [17]. However, the specific effect of non-condensable gas on the heat transfer performance of high-temperature heat pipe

is still relatively small, which has a more important reference role for the application design and performance optimization of high-temperature heat pipe [16, 18].

2. Experimental system

The experimental system consists of three parts: heating equipment, high-temperature heat pipe, temperature measurement and recording output system. Test system diagram and thermocouple measuring point layout are shown in Fig. 1.

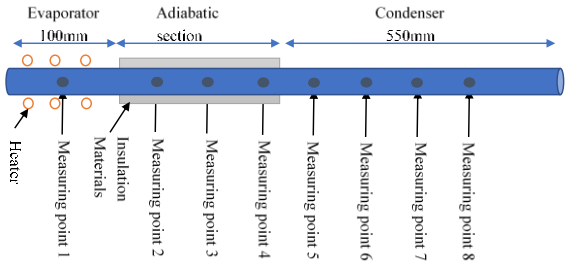

Fig. 1 Test system diagram and thermocouple measuring point layout

The working fluid of high-temperature heat pipe is sodium, and the fill volume is 175 g. The specific parameters of heat pipe are shown in Tab. 1. A series of K-type thermocouples are arranged in the axial direction of the heat pipe to measure the temperature of the high-temperature heat pipe. The location of the thermocouple measuring points is shown in Fig. 1. The temperature values of each measuring point are automatically collected and recorded by the data acquisition instrument.

Table 1 Parameters of sodium heat pipe

Parameter	Numerical value
Heat pipe length (mm)	1000
Length of evaporation section (mm)	100
Length of insulation section (mm)	350
Length of condensing section (mm)	550
Working fluid	sodium
Working fluid filling capacity (g)	175
Wall material	stainless steel
Outer diameter of heat pipe (mm)	32
Inner diameter of heat pipe (mm)	28
capillary wick	stainless steel wire mesh

3. Uncertainty analysis

Reliable temperature and heat flux measurements are vital, so the uncertainty analysis is necessary. The temperature is measured by the K-type thermocouples and recorded by multi-channel data logger. The precision of the calibrated thermocouple is 1°C when the maximum calibrated temperature is 1000°C. The precision of the multi-channel data logger is 0.2%. In this study, the experimental measurement temperature is from environmental

temperature 20℃ to maximum heat pipe temperature of 750°C. Thus, the uncertainty of temperature can be culculate as:

$$\sigma_{\mathrm{t}} = (\sigma_{\mathrm{tc}}^2 + \sigma_{\mathrm{l}}^2)^{1/2} \tag{1}$$

$$\sigma_{\mathrm{tc}} = 0.1\% \tag{2}$$

$$\sigma_{\mathrm{l}} = 0.2\% \tag{3}$$

where σ_{t} is the uncertainty of temperature, σ_{l} is the precision of the multi-channel data logger and σ_{tc} is the precision of the calibrated thermocouple.

4. Results and discussions

For the study on the heat transfer performance of high-temperature heat pipes, typical performances such as start-up performance and temperature uniformity are usually studied. The start-up time of the heat pipe reflects the heat response speed of the heat pipe and temperature uniformity is an important manifestation of the heat transfer effect of high-temperature heat pipes.

The "flat-front startup model" is usually used to predict the startup process of high-temperature heat pipes [19]. The time from the beginning of heating to the formation of a continuous stream of steam at the outlet of the evaporation section is defined as the start-up time. Then the start-up time can be calculated by the following formula:

$$\tau = cl(T_{\mathrm{hw}} - T_{\mathrm{a}})/Q \tag{4}$$

$$c = c_{\mathrm{w}} + \varepsilon c_{\mathrm{s}} + (1-\varepsilon)c_{\mathrm{ws}} \tag{5}$$

where τ is the start-up time of the heat pipe, c is the heat capacity of heat pipe, l is the length of the evaporation section of the heat pipe, T_{hw} is the temperature of hot zone of heat pipe, T_{a} is the temperature of cold zone of heat pipe, Q is the heating power of the heat pipe, c_{w} is the heat capacity of the heat pipe wall, c_{ws} is the heat capacity of the wick, ε is the porosity of capillary wick.

4.1. Effect of inclination angle on performance of high-temperature heat pipe

In the experiment, the performance of high-temperature heat pipe was tested under the same heating power (3000 W) and different inclination angles (0°, 30°, 60° and 90°), and the results are shown in Fig. 2. It shows the temperature variation of sodium heat pipe with different inclination angles. It shows the change of start-up time of heat pipe when the inclination angle of heat pipe increases from 0° to 90° in Fig. 3. It can be seen from Fig. 3 that the influence of inclination angle on start-up time is not very significant, and the fluctuation is

very small. As the inclination angle changes, the start-up time of the heat pipe does not change more than 5%. It can be seen from Eq. (4) that the start-up time is related to the heat capacity and heating power of the heat pipe. When the heating power remains the same, the start-up time is determined by the heat capacity of the heat pipe. The experimental results are consistent with the prediction results of the " flat-front startup model". This conclusion is consistent with the result in [20] that the inclination angle has little effect on the start-up time of the heat pipe.

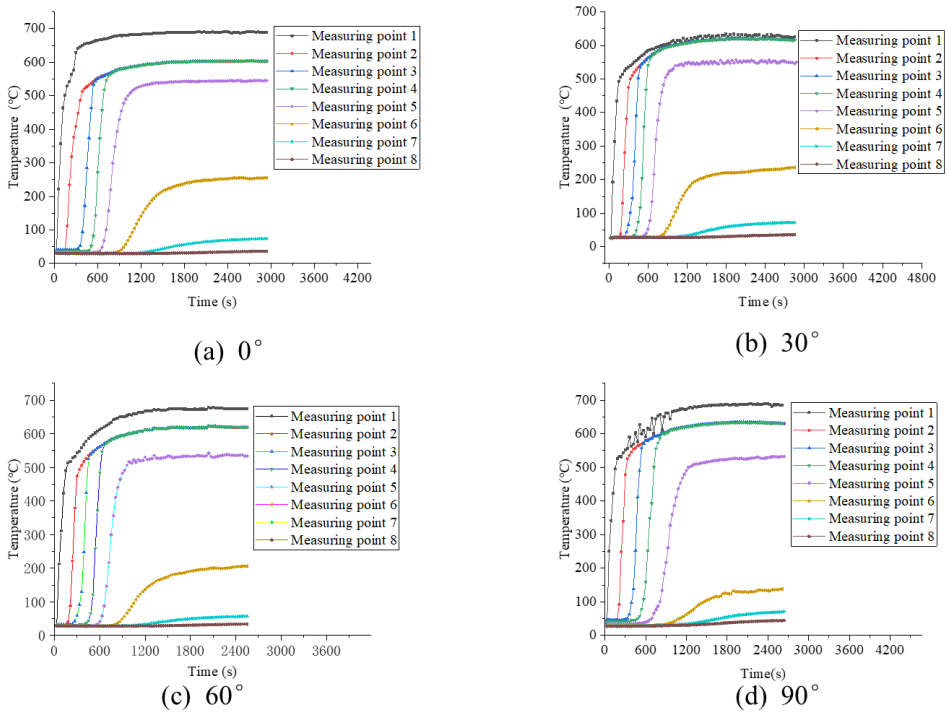

Fig. 2 Temperature variation of 3000 W heat pipe with different inclination angles

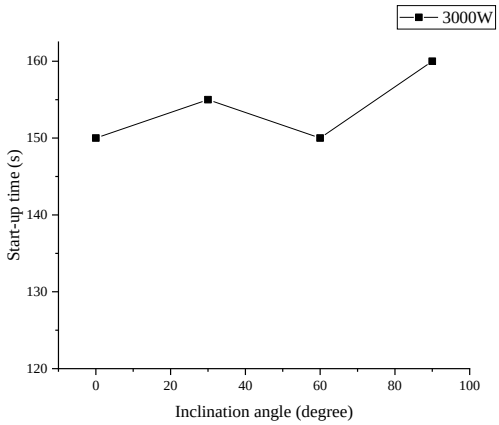

Fig. 3 Start-up time chart of 3000 W heating power with different inclination angles

The axial temperature distribution of heat pipe at different inclination angles is shown in Fig.4. It can be seen from Fig. 4 that with the increase of heat pipe inclination angle, the heat transfer performance of heat pipe first increases and then decreases, and the heat transfer performance is the best when the inclination angle is 30°. Senthil [21] investigated the heat pipe with deionized water as the working fluid and the results showed that the heat pipe at an inclined position of 45° has about 71% higher heat transfer coefficient with minimum thermal resistance when compared to the horizontal and vertical positions. This difference is mainly due to the different structure of the heat pipe.

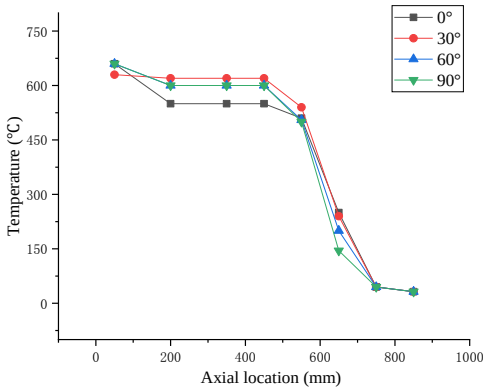

Fig. 4 Axial temperature distribution of heat pipe with different inclination angles at 3000 W heating power

4.2. Influence of non-condensable gas on heat transfer performance of high-temperature heat pipe

From the axial temperature distribution diagram of high-temperature heat pipe shown in Fig.4, it can be seen from Fig. 4 that the heat pipe contains a certain amount of non-condensable gas, which has a certain impact on the heat transfer performance of the heat pipe. It is difficult to completely avoid the non-condensable gas in the process of manufacturing and using the heat pipe[13]. Therefore, it is necessary to consider the influence of non-condensable gas when studying the high-temperature heat pipe. The common analysis model [22] of high-temperature heat pipe does not consider the influence of non-condensable gas.

The heat transfer model of non-condensable gas in heat pipe during steady state operation is usually compared with circuit model [23]. The typical network model of heat pipe is shown in Fig. 5 [15]. The thermal resistances are defined as the ratio between temperature differences and the heat power transferred. In this figure, R_1 and R_9 are related to the external heat exchange phenomena; R_2, R_8 and R_{10} are related to the heat conduction through the tube wall in the axial (evaporator and condenser regions) and longitudinal directions, respectively; R_3 is related to the evaporation, and has two sub regions: the pool boiling resistance, in the evaporator rear region where working fluid accumulates, and the liquid film in the wall; R_4 and R_6 are the thermal resistances associated with the interface liquid–vapor, for the evaporator and condenser, respectively, usually neglected; and, finally,

R_5 is the thermal resistance associated with the vapor flow inside the tube. R_7 is the condensation resistance.

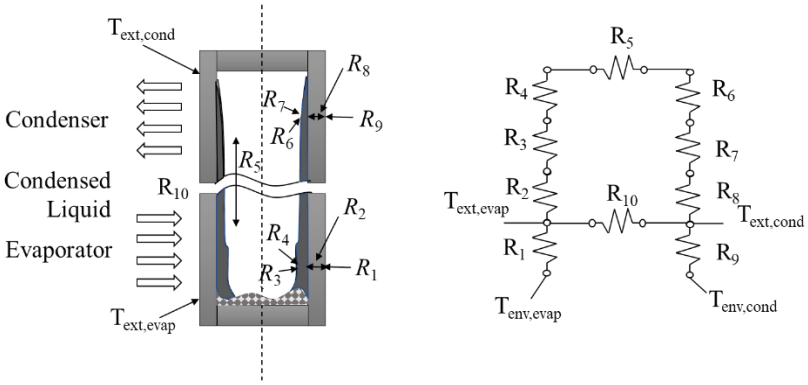

Fig. 5 Typical network model of heat pipe without NCG [15]

Heat is transferred from the outer wall of evaporation section, and transferred to condensation section through axial heat conduction of heat pipe, or radial heat conduction of evaporation section, working fluid evaporation, working fluid flow, working fluid condensation, and radial heat conduction of condensation section finally transfers to condensation section. The temperature of the outer wall of the evaporation section is $T_{ext,\ evap}$, and the temperature of the outer wall of the condensation section is $T_{ext,\ cond}$. $T_{env,\ evap}$ and $T_{env,\ cond}$ are the environment temperature. Considering the existence of non-condensable gas in the heat pipe, the model of the improved heat pipe is shown in Fig.6.

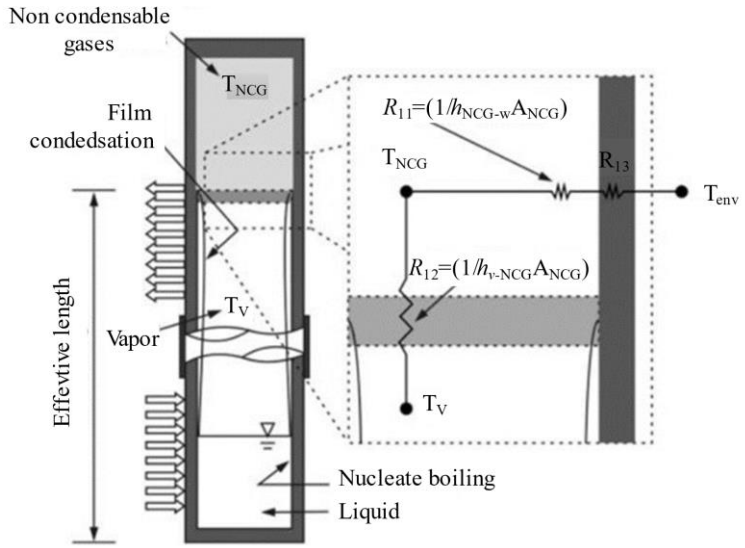

Fig. 6 Heat transfer model of non-condensable gas section of heat pipe containing NCG [15]

After adding non-condensable gas, the condensed gas will form a non-condensable gas section at the tail end of the heat pipe under the action of steam pressure, and a certain interface thermal resistance is considered at the interface between the non-condensable gas

and the condensing section. R_{11} is the interface thermal resistance between the non-condensable gas and the wall of the heat pipe. R_{12} is the interface thermal resistance between the non-condensable gas and the working fluid steam. It can be calculated from the area of the non-condensable gas and the interface heat transfer coefficient according to the calculation formula in the figure. R_{13} is the heat conduction thermal resistance of the heat pipe wall in the non-condensable gas section.

It is generally believed that under the heat flux below the boiling limit of the heat pipe, the phase change of the liquid pool in the heat pipe is mainly evaporation or nucleate boiling. But for the inside of the high-temperature heat pipe, the density of liquid metal, the viscosity and heat capacity of the working fluid are relatively large. So, it is difficult to have severe nuclear boiling. Therefore, it is assumed that the main phase transformation mode in the evaporation section is evaporation [24]. In order to simplify the calculation, the following assumptions are made: the evaporation section is full of liquid, the adiabatic section does not participate in heat transfer and the condensation section is film condensation, forming a uniform film on the pipe wall, the interface between the condensation section and NCG section is plane, and the diffusion and mass transfer between NCG and steam are not considered, as well there is natural convection heat transfer in NCG section.

Then the energy balance equation in part i can be obtained as follows

$$\rho_{\mathrm{i}} A_{\mathrm{i}} \delta_{\mathrm{i}} c_{\mathrm{p,i}} \frac{dT_{\mathrm{i}}}{d\mathrm{t}} = Q_{\mathrm{i,1}} - Q_{\mathrm{i,2}} \tag{6}$$

$$Q_{\mathrm{i,1}} = \lambda_{\mathrm{i}} A_{\mathrm{i}} \frac{T_{\mathrm{i,1}} - T_{\mathrm{i}}}{\delta_{\mathrm{i}}/2} \tag{7}$$

$$Q_{\mathrm{i,2}} = \lambda_{\mathrm{i}} A_{\mathrm{i}} \frac{T_{\mathrm{i}} - T_{\mathrm{i,2}}}{\delta_{\mathrm{i}}/2} \tag{8}$$

where ρ_{i} is the density of part i, A_{i} is the cross-sectional area of part i, δ_{i} is the length in the direction of heat transfer of part i, $c_{\mathrm{p,\,i}}$ is specific heat capacity at constant pressure of part i, T_{i} is the temperature of part i, $T_{\mathrm{i,1}}$ is the hot end temperature in the heat transfer direction of part i, $T_{\mathrm{i,2}}$ is the cold end temperature in the heat transfer direction of part i, t is time, $Q_{\mathrm{i,1}}$ is the input power of part i, $Q_{\mathrm{i,2}}$ is the output power of part i, λ is the thermal conductivity.

Using Newton's interpolation method to solve the simultaneous equations, the temperature distribution solution of the high temperature heat pipe containing non-condensable gas can be obtained.

4.2.1 The effect of non-condensable gas on effective length of the heat pipe

For the high-temperature heat pipe containing a certain amount of non-condensable gas, the steam temperature and pressure in the steam chamber of the heat pipe (except NCG section) has little change, so it is considered that the steam temperature and pressure in the steam chamber are consistent. The saturated steam pressure can be calculated from the steam temperature to get the pressure of the non-condensable gas section. According to the ideal gas

calculation formula, the length calculation formula of non-condensable gas section is as follows:

$$l_{\mathrm{NCG}} = \frac{1}{A_{\mathrm{c}}} \frac{\mathrm{N}_0 \mathrm{R} T_{\mathrm{NCG}}}{P_{\mathrm{NCG}}} \tag{9}$$

$$l_{\mathrm{eff}} = L - l_{\mathrm{NCG}} \tag{10}$$

where L is the total length of the heat pipe, l_{NCG} is the length of the non-condensable gas section of the heat pipe, l_{eff} is the effective length of the heat pipe, N_0 is the number of moles, R is the gas constant (=PV/nT), T_{NCG} is the NCG temperature, A_{c} is the tube cross section area, P_{NCG} is the NCG pressure.

4.2.2 The influence of non-condensable gas on temperature distribution

For the transition section (adiabatic section, the junction of steam and non-condensable gas), the temperature distribution characteristics are similar to the following formula [25]:

$$T_x = \frac{T_{\mathrm{cond}} - T_{\mathrm{NCG}}}{1 + \exp(\frac{x - x_{\mathrm{v-NCG}}}{s_{\mathrm{v-NCG}}})} + \frac{T_{\mathrm{evap}} - T_{\mathrm{cond}}}{1 + \exp(\frac{x - x_{\mathrm{adiab}}}{s_{\mathrm{adiab}}})} \tag{11}$$

where T_{cond}, T_{NCG}, T_{evap} are the temperatures of the condenser, NCG and evaporator, respectively (obtained from the averages of the temperature data in these regions), x is the axial location, $x_{\mathrm{v\text{-}NCG}}$ and x_{adiab} are the positions of the interface vapor–NCG and of the adiabatic section, $s_{\mathrm{v\text{-}NCG}}$ and s_{adiab} are parameters which rule the curve inclination in the concavity change point.

The temperature distribution diagram of the high-temperature heat pipe containing non-condensable gas along the length of the tube is shown in Fig. 7. The picture on the left side of Fig. 7 is the actual measurement of the axial temperature distribution of the heat pipe containing non-condensable gas, and the picture on the right side is the prediction diagram of the theoretical model of the axial temperature distribution of the heat pipe containing non-condensable gas. It can be seen from Fig. 7 that when the high-temperature heat pipe reaches a steady state, three isothermal sections appear at one time along the axial temperature distribution of the heat pipe. They are the evaporation section, the condensation section and the non-condensable gas section. The temperature change from the evaporation section to the condensing section is small, and the temperature from the condensing section to the non-condensable gas section is greatly reduced because there is no mass transfer and the heat transfer is solely dependent on heat conduction.

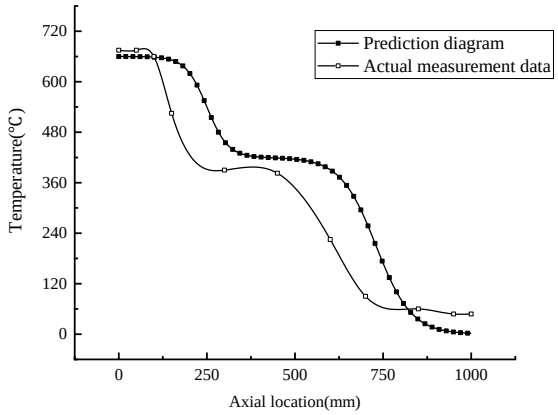

Fig. 7 Temperature distribution along the length of the heat pipe containing NCG

In order to compare the model results with the experimental results, the axial temperature distribution of the high-temperature heat pipe under different heating powers was measured, and the results are shown in Fig. 8. It is shown in Fig. 8 that due to the limitation of the thermocouple measuring point arrangement and the fitting sampling setting in the experiment, some sections of the fitting curve show a wave shape. The adiabatic section is not completely insulated, so an isothermal section also appears in the adiabatic section. The approximate temperature trend is consistent with the model prediction results. The larger the input power, the closer the fitting curve is to the model prediction result. As the input power increases, the steam pressure in the heat pipe increases, the working fluid circulates faster, and the boundary between non-condensable gas and working fluid steam becomes more obvious. It is closer to the assumption that mass transfer is not performed at the interface between the non-condensable gas section and the condensing section in the model. At the same time, it can be concluded from Fig. 8 that the effective length of the heat pipe is about 710 mm.

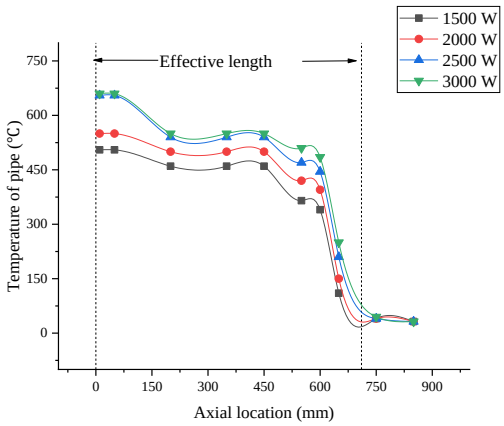

Fig. 8 Fitting curve of axial temperature distribution of heat pipes with different heating power placed horizontally

5. Conclusion

Through experimental research on the sodium working fluid high-temperature heat pipe, the heat transfer performance of the sodium heat pipe under different inclination angles is obtained. A heat transfer model of sodium heat pipe containing non-condensable gas was established to study the effect of non-condensable gas on the heat transfer performance of high-temperature heat pipes. The following conclusions may be made:

1. The inclination angle has no effect on the startup time of high-temperature heat pipes. But when the inclination angle is about 30°, the heat pipe has the best temperature uniformity;

2. The presence of the non-condensable gas will reduce the effective length of the high-temperature heat pipe, increase the thermal resistance and decrease the heat transfer performance;

3. Using the sodium heat pipe heat transfer model containing non-condensable gas established in this article, the length occupied by the non-condensable gas can be judged, and the amount of non-condensable gas contained in the heat pipe can be calculated.

Acknowledgment

The supports of our research program by National Natural Science Foundation of China (No. 11802125) and Jiangsu Province Key Laboratory of Aerospace Power System (China) are greatly appreciated. We are very indebted to the anonymous reviewers for their invaluable suggestions.

Nomenclature

A – The cross-sectional area of the heat pipe, [m^2]

c – Heat capacity of heat pipe, [$Jm^{-1}K^{-1}$]

c_p – specific heat capacity at constant pressure, J/K;

c_w – The heat capacity of the heat pipe wall, [$Jm^{-1}K^{-1}$]

c_{ws} – The heat capacity of the wick, [$Jm^{-1}K^{-1}$]

L – The length of the heat pipe, [m]

l – The length of the evaporation section of the heat pipe, [m]

l_{eff} – The effective length of the heat pipe, [m]

l_{NCG} – The length of the non-condensable gas section of the heat pipe, [m]

N_0 – The number of moles, [mol]

P_{adiab} – The pressure of non -gaseous gas, [Pa]

P_{NCG} – The NCG pressure, [K].

Q – The heating power of the heat pipe, [W]

R – Gas constant (=PV/nT), [$Jmol^{-1}K^{-1}$]

s_{adiab} – The length of adiabatic section, [m]

$s_{v\text{-}NCG}$ – The length of the transition section between steam and non-condensable gas, [m]

t – Time, s;

T_a – The temperature of cold zone of heat pipe, [K]

T_{hw} – The temperature of hot zone of heat pipe, [K]
T_{cond} – The temperature of condensation section, [K]
T_{evap} – The temperature of the evaporation section, [K]
T_{NCG} – The temperature of the non-condensable gas section, [K]
x – Axial location, [m]
$x_{v\text{-}NCG}$ – The positions of the interface vapor–NCG;
x_{adiab} – The positions of the adiabatic section;

Greek Symbols
δ – Length in the direction of heat transfer within the computing unit, [m]
ε – The porosity of capillary core, [–]
λ – The thermal conductivity, [$Wm^{-1}K^{-1}$]
ρ – Density, [kg/m^3]
σ_l – The precision of the multi-channel data logger, [–]
σ_t – The uncertainty of temperature;
σ_{tc} – The precision of the calibrated thermocouple, [–]
τ – The start-up time of the heat pipe, [s]

References

[1] Lu N., *et al.*, Experimental Study on Gradient Pore Size Capillary Wicks, *Heat Transfer Research, 53.* (2022), 7, pp. 57-75, DOI No. 10.1615/HeatTransRes.2022040095

[2] Lu N., *et al.*, Research progress and prospect of heat pipe capillary wicks. *Frontiers in heat and mass transfer, 18*. (2022), 24, DOI No. http://dx.doi.org/10.5098/hmt.18.24

[3] Li J., *et al.*, Experimental study on evaporation-capillary pumping flow in capillary wick and working fluid system, Thermal Science, 25. (2021), 1A, pp. 367-375, DOI No. https://doi.org/10.2298/TSCI180918413L

[4] Werner, T.C., *et al.*, Experimental analysis of a high temperature water heat pipe for thermal storage applications, *Thermal Science and Engineering Progress*, *19*. (2020), p. 100564, DOI No. https://doi.org/10.1016/j.tsep.2020.100564

[5] Xu, R., *et al.*, Testing and Modeling of the Dynamic Response Characteristics of Pulsating Heat Pipes during the Start-up Process, *Journal of Thermal Science*, *28*. (2018), 1, pp. 72-81, DOI No. 10.1007/s11630-018-1032-1

[6] Chidambaranathan, S., Rangaswamy, S., Experimental investigation of higher alcohols as self-rewetting fluids in closed loop pulsating heat pipes, *Thermal Science*, *25*. (2021), 1 Part B, pp. 781-790, DOI No. 10.2298/tsci200509347c

[7] Xudong, S.U.N., *et al.*, RESEARCH ON MULTI-STAGE HEATING METHOD OF HIGH SPEED RAILWAY EMERGENCY TRACTION BATTERY SYSTEM BASED ON FLAT HEAT PIPE, *Thermal Science*, *25*. (2021), 2A, pp. 1203-1215, DOI No. 10.2298/TSCI200118172S

[8] Mahdavi, M., *et al.*, Experimental study of the thermal characteristics of a heat pipe, *Experimental Thermal and Fluid Science*, *93*. (2018), pp. 292-304, DOI No. https://doi.org/10.1016/j.expthermflusci.2018.01.003

[9] Ping, Y., *et al.*, Startup performance of high-temperature sodium heat pipe with triangular groove wick, *Journal of Nanjing TECH University, 37*. (2015), 01, pp. 99-103, DOI No. 10.3969/j.issn.1671-7627.2015.01.018

[10] Li, D., *et al.*, Test study on ISO thermal and heat conducting performance of high-temperature heat pipe in solar energy receiver, *Thermal power generation*, *39*. (2010), 03, pp. 40-44+48, DOI No. 10.3969/j.issn.1002-3364.2010.03.040

[11] Yan, S., *et al.*, Heat transfer characteristics of high temperature heat pipe with triangular grooved wick under variable heat fluxes, *CIESC Journal*, *65*. (2014), 10, pp. 3829-3837, DOI No. 10.3969/j.issn.0438-1157.2014.10.012

[12] Hack, N., *et al.*, Ceramic Heat Pipes for High Temperature Application, *Energy Procedia*, *120*.(2017), pp. 140-148, DOI No.https://doi.org/10.1016/j.egypro.2017.07.147

[13] Jiang,H., *et al.*, Effect of non-condensable gas on performance of two-phase thermal control devices for spacecraft, *Spacecraft Engineering*, *23*. (2014), 06, pp. 114-121, DOI No. 10.3969/j.issn.1673-8748.2014.06.019

[14] Ochterbeck, J.M., Modeling of Room-Temperature Heat Pipe Startup from the Frozen State, *Journal of Thermophysics and Heat Transfer*, *11*. (1997), 2, pp. 165-172, DOI No. 10.2514/2.6248

[15] Mantelli, M.B.H., *et al.*, Performance of naphthalene thermosyphons with non-condensable gases – Theoretical study and comparison with data, *International Journal of Heat and Mass Transfer*, *53*. (2010), 17-18, pp. 3414-3428, DOI No. 10.1016/j.ijheatmasstransfer.2010.03.041

[16] Tarau, C., *et al.*, Thermal Management System for Long-Lived Venus Landers, *9th Annual International Energy Conversion Engineering Conference*. (2011), DOI No. 10.2514/6.2011-5643

[17] Joung, W., *et al.*, Hydraulic operating temperature control of a loop heat pipe, *International Journal of Heat and Mass Transfer, 86*. (2015), pp. 796-808, DOI No. 10.1016/j.ijheatmasstransfer.2015.03.056

[18] El-Genk, M., Tournier, J.-M., Challenges and fundamentals of modeling heat pipes' startup from a frozen state, *AIP Conference Proceedings*, *608*. (2002), 1, p. 127, DOI No. 10.1063/1.1449717

[19] Cao, Y.,A. Faghri, Closed-form analytical solutions of high-temperature heat pipe startup and frozen startup limitation, *Journal of Heat Transfer, 114*. (1992), pp. 1028-1035, DOI No. 10.1115/1.2911873

[20] Tao, N., *et al.*, Properties of high-temperature heat pipe and its experimental, *ACTA AERONAUTICAET ASTRONAUTICA SINICA*, 37(2016), S1, pp. 59-65, DOI 10.7527/S1000-6893.2016.0165

[21] Chandrasekaran, S.K., Srinivasan, K., EXPERIMENTAL STUDIES ON HEAT TRANSFER CHARACTERISTICS OF SS304 SCREEN MESH WICK HEAT PIPE, *Thermal Science*. (2017), pp. S497-S502, DOI No. 10.2298/TSCI17S2497C

[22] Bao,H., *et al.*, Steady Numerical Analysis of Potassium Heat Pipe, *Atomic Energy Science and Technology*, *44*. (2010), 05, pp. 553-557

[23] Groll, M.,S. Rosler, Operation Principles and Performance of Heat Pipes and Closed Two-Phase Thermosyphons, *Journal of Non-Equilibrium Thermodynamics*, *17*. (1992), pp. 91-151, DOI No. 10.1515/jnet.1992.17.2.91

[24] Yan, S., *et al.*, Simulation and experimental analysis on heat transfer characteristics of alkali metal heat pipe, *ACTA ENERGIAE SOLARIS SINICA*, *37*. (2016), 03, pp. 644-650, DOI No. 10.3969/j.issn.0254-0096.2016.03.018

[25] Hoehler, F.K., Logistic equations in the analysis of S-shaped curves, *Computers in Biology and Medicine*, *25*. (1995), 3, pp. 367-371, DOI No. https://doi.org/10.1016/0010-4825(95)00013-T

Paper submitted: 07 February 2022

Paper revised: 21 August 2022

Paper accepted: 22 August 2022